THE JOURNAL OF BIOLOGICAL CHEMISTRY VOL. 284, NO. 18, pp. 12020–12030, May 1, 2009

Mice Lacking the Extracellular Matrix Protein WARP Develop Normally but Have Compromised Peripheral Nerve Structure and Function*

Received for publication, September 9, 2008, and in revised form, January 16, 2009 Published, JBC Papers in Press, March 11, 2009, DOI 10.1074/jbc.M806968200

Justin M. Allen[‡], Laura Zamurs[‡], Bent Brachvogel[‡§], Ursula Schlötzer-Schrehardt[¶], Uwe Hansen[‖], Shireen R. Lamandé[‡], Lynn Rowley[‡], Jamie Fitzgerald[‡], and John F. Bateman[‡ ‡‡1]**

*From the [‡]Murdoch Children's Research Institute and [‡‡]Department of Paediatrics, University of Melbourne, Royal Children's Hospital, Parkville, Victoria 3052, Australia, [§]Center for Biochemistry, Medical Faculty, University of Cologne D-50931,Germany, [¶]Department of Ophthalmology, University Erlangen-Nürnberg, Erlangen D-91054, Germany, **Department of Orthopaedics and Rehabilitation, Oregon Health and Science University, Portland, Oregon 97239, and [‖]Institute for Physiological Chemistry and Pathobiochemistry, University Hospital of Muenster, Muenster D-48149, Germany*

WARP is a recently identified extracellular matrix molecule with restricted expression in permanent cartilages and a distinct subset of basement membranes in peripheral nerves, muscle, and the central nervous system vasculature. WARP interacts with perlecan, and we also demonstrate here that WARP binds type VI collagen, suggesting a function in bridging connective tissue structures. To understand the *in vivo* function of WARP, we generated a WARP-deficient mouse strain. WARP-null mice were healthy, viable, and fertile with no overt abnormalities. Motor function and behavioral testing demonstrated that WARP-null mice exhibited a significantly delayed response to acute painful stimulus and impaired fine motor coordination, although general motor function was not affected, suggesting compromised peripheral nerve function. Immunostaining of WARP-interacting ligands demonstrated that the collagen VI microfibrillar matrix was severely reduced and mislocalized in peripheral nerves of WARP-null mice. Further ultrastructural analysis revealed reduced fibrillar collagen deposition within the peripheral nerve extracellular matrix and abnormal partial fusing of adjacent Schwann cell basement membranes, suggesting an important function for WARP in stabilizing the association of the collagenous interstitial matrix with the Schwann cell basement membrane. In contrast, other WARP-deficient tissues such as articular cartilage, intervertebral discs, and skeletal muscle showed no detectable abnormalities, and basement membranes formed normally. Our data demonstrate that although WARP is not essential for basement membrane formation or musculoskeletal development, it has critical roles in the structure and function of peripheral nerves.

WARP (von Willebrand A domain-related protein) is a recently described member of the von Willebrand factor type A domain (VWA[2] domain) superfamily of extracellular matrix (ECM) molecules, adhesion proteins, and cell surface receptors (for review, see Ref. 1). The WARP protein is encoded by the *Vwa1* (von Willebrand factor A domain-containing 1) gene and comprises a single N-terminal VWA domain containing a putative metal ion-dependent adhesion site (MIDAS) motif, two fibronectin type III repeats, and a unique C-terminal domain that contributes to WARP multimer formation (2, 3). Like many other VWA domain-containing extracellular molecules, WARP was predicted to participate in protein-protein interactions and in the formation of supramolecular structures. Recently WARP has been shown to interact with the heparan sulfate proteoglycan perlecan (3), and in the present study we identify type VI collagen as a ligand for WARP.

WARP has a restricted distribution in developing cartilage tissues, where it is expressed at sites of joint cavitation and articular cartilage formation rather than cartilage structures that will undergo endochondral ossification (3). In adult tissues, WARP is highly restricted to the chondrocyte pericellular matrix in articular cartilage and fibrocartilages, where it colocalizes with perlecan and collagen VI (3). Several of the major basement membrane components have been found in the chondrocyte pericellular matrix, suggesting that this structure may be the functional equivalent of a basement membrane in cartilage tissues (4). Consistent with this hypothesis, recent data from our laboratory have demonstrated that WARP is a component of the basement membrane in a limited subset of tissues including the apical ectodermal ridge, the endomysium surrounding muscle fibers, the vasculature of the central nervous system, and the endoneurium of peripheral nerves (5). The principal components of basement membranes are type IV collagen, laminins, nidogens, and proteoglycans including perlecan; however, the composition, structure, and biological properties of basement membranes can differ considerably between different tissues (6, 7). Different isoforms of the major components contribute to the heterogeneity of basement membranes, but the contribution of quantitatively minor components to particular subtypes of basement membranes and their interactions with surrounding cells and ECM structures are poorly understood (8, 9).

We, therefore, have generated mice with a targeted disruption of the WARP locus to determine the consequences of

* This work was supported by grants from the National Health and Medical Research Council of Australia, Muscular Dystrophy Association Grant 4076, and the Murdoch Children's Research Institute.

[1] To whom correspondence should be addressed: Murdoch Children's Research Institute, Royal Children's Hospital, Parkville, Victoria 3052, Australia. Fax: 61-3-8341-6429; E-mail: john.bateman@mcri.edu.au.

[2] The abbreviations used are: VWA, von Willebrand factor type A; ECM, extracellular matrix; PBS, phosphate-buffered saline; CHAPS, 3-[(3-cholamidopropyl)dimethylammonio]-1-propanesulfonic acid.

WARP deficiency on skeletal development and basement membrane formation. The homozygous null mice are viable, fertile, and do not exhibit overt abnormalities compared with wild type littermates. Neurological testing revealed that WARP-null mice exhibit a delayed response to acute painful stimulus and a disturbance in fine motor coordination, although general motor function is not impaired. Consistent with these findings, immunohistochemical analysis of peripheral nerves from WARP-null mice revealed that the collagen VI microfibrillar matrix was severely reduced and mislocalized compared with wild type mice. Furthermore, electron microscopic examination of the sciatic nerve demonstrated a reduction in the collagen I ECM and the unusual partial fusing of the basement membranes of neighboring axons. These data suggest an important role for WARP in organizing the peripheral nerve ECM and provides evidence for tissue-specific differences in the role of WARP in the assembly and/or integration of the ECM. In addition, our studies provide further evidence for the critical role of ECM structure and organization in nerve function.

EXPERIMENTAL PROCEDURES

Generation of a WARP-deficient Mouse Strain—Heterozygous WARP knock-out mice, termed *Vwa1*$^{+/-}$, were generated on a C57BL/6 background under contract by Ozgene Pty Ltd., Western Australia. This strain has a targeted replacement of the coding region of the *Vwa1* gene by the β-galactosidase reporter gene containing a mouse nuclear localization sequence as well as a neomycin selection cassette (5). Heterozygous mice with germline transmission identified by Southern analysis were provided by Ozgene and were mated to establish a breeding colony. All mouse experiments were approved by the Animal Ethics Committees of the Murdoch Children's Research Institute or the Howard Florey Institute (behavioral testing).

Genotyping—Genotyping was performed by PCR of genomic DNA prepared by proteinase K digestion of tail biopsies taken at weaning. The primers *intron4up* 5′-TGTTGTTAGAGTCCGGGTCA and *exon4dw* 5′-GGAGCAAGGTGTCATGCAG detected the wild type PCR product (196 bp), and primers *lacZ2up* 5′-GCCAGTTTGAGGGGACGACGACAG and *promo1dw* 5′-TCACGGTAGGAGGGCAAGT amplified the mutant product (367 bp). Multiplex genotyping PCR reactions containing both of the above primer pairs consisted of initial denaturation at 94 °C for 5 min, 35 cycles of denaturation (94 °C for 1 min), annealing (63 °C for 30 s), and elongation (72 °C for 30 s), and 7 min of elongation at 72 °C.

RNA Extraction and Northern Blotting—Total RNA was extracted from spinal cord and brain from 20-week-old mice using the guanidine isothiocyanate method (10). The RNA was phenol:chloroform-extracted and further purified using the RNeasy kit (Qiagen) including an RNase-free DNase digestion step (Qiagen). Denatured RNA samples (5 μg) were fractionated by electrophoresis through 0.8% agarose-formaldehyde gel and transferred to nitrocellulose (Schleicher & Schuell) overnight by capillary transfer. RNA was immobilized to the membrane by baking at 80 °C under vacuum for 1 h. Northern blots were prehybridized with ExpressHyb (Ambion) solution containing 100 μg/ml sheared and denatured fish sperm DNA for 1 h at 68 °C before hybridization for 2 h at 68 °C with a [α-^{32}P]dCTP-labeled 1.1-kilobase cDNA probe complementary to a region from exons 3 to 4 of the *Vwa1* gene (Megaprime labeling kit, Amersham Biosciences). Blots were stripped by boiling in 0.5% SDS for 10 min and reprobed with a cDNA probe for β-actin (Ambion) to control for loading.

Protein Extraction and Immunoblotting—Sciatic nerves were dissected and snap-frozen in liquid nitrogen. Frozen nerve tissue was ground into powder and extracted overnight at 4 °C with agitation in buffer containing 4 M guanidine hydrochloride, 50 mM sodium acetate (pH 5.8), 10 mM EDTA, and Complete Protease Inhibitors (Roche Applied Science). The supernatant was clarified by centrifugation at 13,000 rpm for 20 min at 4 °C and quantitated using the BCA Protein Assay (Pierce) following the manufacturer's instructions. For SDS-PAGE, 10 μg of each extract was precipitated with 90% ethanol overnight, and the pellet was washed with 70% ethanol and resuspended in SDS loading buffer. After denaturation at 99 °C for 5 min and reduction with 50 mM dithiothreitol, samples were resolved on a 10% polyacrylamide gel and transferred to Hybond-LFP membrane (GE Healthcare). Duplicate blots were probed with a 1:8000 dilution of a polyclonal sheep antibody raised to full-length recombinant WARP (5) or a monoclonal β-actin antibody (Sigma). Bound antibodies were detected with AlexaFluor 647-conjugated donkey anti-goat, which also specifically binds sheep IgG, or 594-conjugated donkey anti-mouse antibodies (Invitrogen) and visualized with a Typhoon 9400 PhosphorImager (Amersham Biosciences).

Immunohistochemistry and Histology—Tissues for histology were dissected and fixed in 10% formalin overnight at 4 °C. Skeletal tissues were decalcified for 24–48 h in Immunocal (Decal) before dehydration through graded ethanol solutions and embedding in paraffin. Microtome sections (5 μm) of skeletal tissues were stained with 0.1% (w/v) toluidine blue O in 0.1 M sodium acetate buffer (pH 4.0), for 10 min and counterstained with Fast Green FCF with 3 min. Muscle tissues were frozen directly in liquid nitrogen-cooled isopentane, then mounted in Tissue Tek OCT compound at −20 °C and sectioned (10 μm) with a Leica CM3050 cryostat for hematoxylin and eosin staining.

Tissues for immunohistochemistry were fixed in 4% paraformaldehyde in PBS, decalcified in PBS with 7% (w/v) EDTA if required, and embedded in Tissue Tek OCT compound by freezing in liquid nitrogen-cooled isopentane. Gastrocnemius muscle samples were snap-frozen in liquid nitrogen. Cartilage cryosections (10 μm) were digested with 0.2% hyaluronidase (bovine, type IV- Sigma), and all sections were blocked and permeabilized with PBS containing 1% bovine serum albumin and 0.1% Triton-X100 for 1 h, then immunolabeled overnight at 4 °C.

WARP was immunolabeled with a rabbit anti-C-terminal domain polyclonal antibody or with a sheep polyclonal antibody raised to full-length recombinant WARP (3, 5). Perlecan was detected with rat anti-perlecan monoclonal antibody (A7L6, Abcam). Collagen VI was immunolabeled with an affinity-purified rabbit anti-human collagen VI polyclonal antibody (Fitzgerald Industries) or with rabbit polyclonal antibodies

raised to recombinant α1(VI) chain or human pepsinized collagen VI (11, 12). Control sections were probed with preimmune serum or with secondary antibodies only. Bound antibodies were detected using Alexa-Fluor-conjugated donkey anti-sheep 488, donkey anti-rabbit 594, or donkey anti-rat 594 secondary antibodies (Invitrogen), and slides were washed in PBS and mounted with Fluorsave (Calbiochem). Immunofluorescence images were visualized with a Leica Diaplan microscope, and laser-scanning confocal microscopy was performed using a Leica TCS SP2 SE confocal microscope. Paired images from wild type and mutant mice were collected with the same exposure times and gain settings except where indicated. Images were processed for pseudocolor where required and for brightness contrast using Adobe Photoshop 6.0; all paired images from wild type and mutant mice were processed identically.

Motor Function Testing of Mutant Vwa$^{-/-}$ and Wild Type Mice—Behavioral testing of wild type and mutant mice was performed by the Integrative Neuroscience Facility, Howard Florey Institute, Melbourne, Australia. Testing was performed on 12 male 11-week-old mice for each genotype, and mice were allowed to acclimatize for 8 days before testing.

Grip Strength Test—Each mouse was allowed to grasp the grid of the apparatus (Bioseb) with its forelimbs and pull gently until it released its grip. The maximum amount of force exerted in grams was recorded. This was repeated 5 times with a 30-s interval between trials, and the average reading was calculated. The mice were then placed on the grid to allow them to grasp with all limbs. They were gently pulled until they released their grip. The maximum amount of force exerted (g) was recorded. This was repeated 5 times with a 30-s interval between each trial, and the average reading was recorded.

Running Wheel Test—Each mouse tested was individually housed in a home cage with a running wheel for 7 days. The running wheel lids were fitted with digital magnetic counters (model BC 800; Sigma sport). The following parameters were recorded at the same time (between 8 a.m. and 12 p.m.) on a daily basis: the distance traveled (km), the average speed (km/h), the amount of time the wheel rotated (h), and the maximum speed reached (km/h). The counter was reset daily, and the running wheel lids were swapped from one cage to another. All animals were supplied with food and water *ad libitum* for the duration of the test.

Locomotor Activity Tests—This test is conducted in the Truscan locomotor system that consists of a plexiglass cage (40 × 27.5 × 27.5 cm) with 2 sensor rings to detect the movement of the animal under low conditions of lighting. Movements in both the horizontal and vertical planes were recorded. A single mouse was placed in each locomotor cell, and recordings made every 500 ms for the duration of the test. The data were collated into 5-min time-bins for 30 min. The locomotor activity cells were cleaned with 70% ethanol between each mouse. Parameters measured included time spent moving, distance moved, and the number of entries into the vertical plane (rearing). Each mouse was tested for one single 30-min period in the locomotor cell, and data, therefore, reflect response to a novel environment rather than habituated activity.

Rotarod Test—Mice were trained to stay on the rotarod (5-chamber accelerating Mouse Rota-rod, Ugo Basile) undergoing three 2-min training trials, with a 15-min break between each trial. In the first two trials the rotarod was set to rotate at a constant speed of 4 rpm. For the third trial the rotarod operated at an accelerating speed from 4 rpm to a maximum of 40 rpm. The test consisted of two 2-min trials and a final 5-min trial, all of which were at an accelerating speed (4–40 rpm over 5 min). The latency to fall off was measured for each trial. Mice had a 15-min break between each trial. All data were expressed as a percentage of total time of trial. The data analyzed were from the final 5-min trial.

Ledged Beam Test—The ledged beam test consisted of a clear Perspex runway. The lower end was 44-mm wide and narrowed gradually to 1 mm over 1 meter. The beam was designed so that there was a gradual incline (15 degrees) which the mice walk up into a darkened box containing home cage bedding. The beam was brightly lit to encourage the mouse to "escape" to the dark home cage. The final 33 cm of the beam was videotaped. The distance marker where the first foot fault occurs was noted; the higher this value, the wider the beam is at the point where the mouse faults. The number of steps made on the last 33 cm of the beam and number of foot faults for each limb were recorded. A foot fault was identified when one of the mouse limbs was placed on the supporting ledge (not on the beam) to facilitate the mouse passage along the beam.

Hotplate Test—The hotplate (Harvard Instruments) was heated to 55 °C, and the mouse was placed in the chamber on to the hotplate. The latency (in seconds) to distressful behavior, such as paw licking and squeaking was timed.

Statistical Analysis—Data were analyzed using SPSS (Version 15.0) software, with differences considered statistically significant at $p < 0.05$. Grip strength, hotplate test, and locomotor activity were analyzed by independent samples *t* test. For the rotarod test, overall performance was subjected to the Mann-Whitney *U* test on the average of three trials, and the percentage of latency to fall off the accelerating rotarod was analyzed by independent sample *t* test. In the ledged beam test, the Mann-Whitney *U* test was used to determine whether there was a difference in the number of steps and in the number of foot faults for the left front and left hind. The distance marked of the first foot fault and number of foot faults for right front and right hind paws were subjected to independent sample *t* tests.

Purification of Collagen VI—Native collagen VI was extracted from bovine cornea. Two frozen cornea were crushed into a fine powder by homogenization under liquid nitrogen. Material was then resuspended in 10 ml of NET buffer (50 mM Tris-HCl (pH 7.5), 150 mM NaCl, 5 mM EDTA, 1% (v/v) Nonidet P-40, 0.1% (w/v) CHAPS) containing protease inhibitors (1 mM 4-(2-aminoethyl)benzenesulfonyl fluoride, 20 mM *N*-ethylmaleimide). After incubation at 4 °C for 2 h, insoluble material was pelleted via centrifugation at 15,000 × *g* for 5 min. The pellet was washed twice with NET buffer and twice with collagenase buffer (50 mM Tris-HCl (pH 7.5), 400 mM NaCl, 10 mM $CaCl_2$). The insoluble material was then resuspended in 10 ml of collagenase buffer containing 2500 units of collagenase (CLSPA, Worthington) per g of cornea, 1300 units of hyaluronidase/g of cornea, 1 mM 4-(2-aminoethyl)benzenesulfonyl fluoride, and

20 mM *N*-ethylmaleimide. Digestion proceeded for 20 h at room temperature. Insoluble material was then removed from the preparation by centrifugation at room temperature at 15000 × *g* for 5 min. Material was stored at 4 °C until required.

One ml of collagenase-digested bovine cornea preparation was loaded onto a CL2B (GE Healthcare) column (150 ml) pre-equilibrated with 50 mM Tris-HCl (pH 7.5), 150 mM NaCl, 5 mM EDTA. Protein was eluted at 0.5 ml/min, and 3-ml fractions were collected. The presence of collagen VI in the resulting fractions was determined after SDS-PAGE analysis and silver staining.

Fractions containing collagen VI were pooled (~9 ml per run) and concentrated using Vivaspin 20-ml 100-kDa cut-off centrifugation units. Concentrated material was then buffer-exchanged into PBS using the same centrifugation units.

Production and Purification of WARP—HEK-293 cells were transfected with a pCEP4 vector (Invitrogen) containing full-length human WARP constructed with an N-terminal His_6 tag using the Amaxa Biosystems Nucleofector kit V (VCA-1003). Cells were grown in Dulbecco's modified Eagle's medium containing 10% (v/v) fetal bovine serum, and transfected cells were selected with hygromycin B (250 μg/ml). Transfected cells were grown to confluency in 175-cm^2 tissue culture flasks in growth medium (Dulbecco's modified Eagle's medium + 10% (v/v) fetal bovine serum). Once confluent, medium was removed, and cells were washed three times with PBS before adding starve media (Dulbecco's modified Eagle's medium). Conditioned media was collected every 48–72 h, and protease inhibitors were added (1 mM 4-(2-aminoethyl)benzenesulfonyl fluoride, 20 mM *N*-ethylmaleimide). Cellular debris was removed by centrifugation at 15000 × *g* for 20 min at 4 °C. The supernatant was stored at 4 °C until required.

Before purification, WARP-conditioned media was dialyzed against buffer A (20 mM phosphate (pH 7.4), 0.5 M NaCl) overnight at 4 °C. Material was then filtered (0.22 μm), and the concentration of imidazole was adjusted to 30 mM. Conditioned media was then loaded at 1 ml/min onto a 1-ml HiTrap Chelating column (GE Healthcare) that was pre-equilibrated in buffer A containing 30 mM imidazole and pre-charged with nickel. The column was washed with buffer A, and protein was eluted at 1 ml/min over a 20-column volume linear gradient of buffer B (20 mM phosphate (pH 7.4), 0.5 M NaCl, 0.5 M imidazole). One-ml fractions were collected and analyzed for the presence of WARP by SDS-PAGE and silver staining.

Biacore Interaction Studies—The interaction between WARP and collagen VI was investigated using a Biacore 3000 (Biacore Life Sciences). Experiments were performed at 25 °C with HEPES-buffered saline buffer (10 mM HEPES (pH 7.4), 3.4 mM EDTA, 0.15 M NaCl, 0.005% (v/v) Tween 20). Purified proteins were immobilized to a CM5 sensor chip at a flow rate of 5 μl/min after activation of the chip surface with a 35-μl mixture of 200 mM *N*-ethyl-*N*′-dimethylaminopropyl-carbodiimide and 50 mM *N*-hydroxysuccinimide. Collagen VI (25 μg/ml) in 10 mM sodium acetate (pH 3.8) and WARP (30 μg/ml) in 5 mM sodium malate (pH 6.0) were coupled to the activated chip. Remaining active groups were blocked with 35 μl of 1 M ethanolamine-HCl (pH 8.5). A control surface containing no immobilized ligand was prepared by activation and blocking in the absence of ligand. Immobilization resulted in 14,000 resonance units of collagen VI (14 ng/mm^2) and 8,000 resonance units of WARP (8 ng/mm^2).

WARP diluted in HEPES-buffered saline buffer was injected over the collagen VI surface at 5 μl/min for 3 min. Binding sites were regenerated using a 12-s pulse of 30 mM NaOH at 50 μl/min. Reciprocal binding was shown by injecting collagen VI (120 μg/ml) over immobilized WARP at 5 μl/min for 3 min. Regeneration of the binding sites was achieved with a 12-s pulse of 10 mM glycine (pH 2.5) at 50 μl/min.

The association (K_A) and dissociation (K_D) rate constants were determined using local fitting to the equation for 1:1 Langmuir binding in the BIAevalution 4.1 software (Biacore). A collagen VI surface of 6000 resonance units (6 ng/mm^2), prepared as described above, was used to determine these rate constants.

Ultrastructural Analysis—Sciatic nerves were fixed in 2.5% glutaraldehyde in 0.1 M phosphate buffer (pH 7.4) for 24 h at 4 °C, post-fixed in 1% buffered osmium tetroxide, and processed for embedding in epoxy resin (Fluka/BioChemika). Ultra thin sections were analyzed by transmission electron microscopy (LEO 906E, Oberkochen; Germany) as described previously (13).

Analysis of Skeletal Morphology—The skeletal morphology of newborn mouse littermates from heterozygous *Vwa1*$^{+/-}$ intercrosses was assessed by Alizarin red and Alcian blue staining for bone and cartilaginous structures. The mice were euthanized, skinned, eviscerated, and fixed in 95% ethanol overnight before 24 h of staining of cartilage structures with 0.015% Alcian blue 8GX in 80 ml of 95% ethanol with 20 ml of acetic acid. After extensive washing in 95% ethanol, tissues were cleared in 1% KOH, and bone structures were stained with 0.5% Alizarin red in 2% KOH overnight. Skeletons were then cleared and preserved in progressive solutions of 2% KOH:glycerol from 80:20, 60:40, 40:60, and 20:80 for storage and photography using a Leica Wild MZ8 microscope.

RESULTS

Generation of WARP-deficient Mice—The gene targeting vector was designed to disrupt the *Vwa1* gene by replacing all four exons with an in-frame insertion of the β-galactosidase reporter gene containing a nuclear localization sequence and a neomycin selection cassette (Fig. 1*A*). The expression of the reporter gene from the *Vwa1* locus in *Vwa*$^{+/-}$ mice recapitulated WARP expression in wild type mice (5). Litters generated by intercrosses between heterozygous *Vwa*$^{+/-}$ mice were genotyped by PCR of tail biopsy genomic DNA samples (Fig. 1*B*). The mutant allele was inherited in the expected Mendelian ratios (25% +/+:51% +/−:24% −/−), and homozygous WARP-null mice were viable, fertile, had indistinguishable growth rates from wild type littermates, and displayed no overt abnormalities.

The ablation of WARP expression was confirmed by mRNA and protein detection methods. Northern blot analysis of total RNA extracted from spinal cord and brain demonstrated that the WARP transcript is undetectable in homozygous mutant mice (Fig. 1*C*). WARP protein was undetectable in nerve lysates by immunoblotting (Fig. 1*D*) and in sections of sciatic nerve by immunofluorescence staining (Fig. 1*E*).

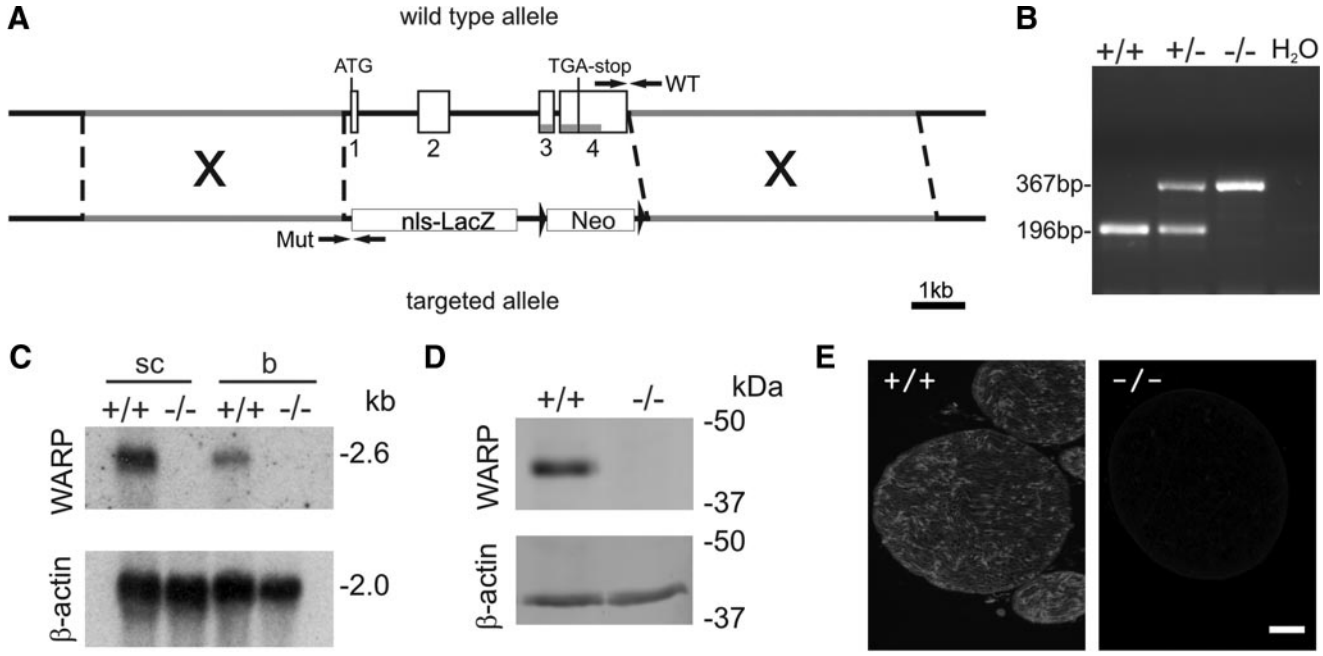

FIGURE 1. **Targeted inactivation of the *Vwa1* gene encoding WARP.** *A*, schematic diagrams of the wild type allele and targeted allele are shown. Exons (*boxes*) are numbered, and the initiation and termination codons are indicated. The *gray underline* in exons 3 and 4 indicates the region of the Northern probe used in *C*. In the targeted allele the nuclear-localized lacZ (*nls-LacZ*) and neomycin cassettes are *highlighted*, and regions of homology are shaded in *gray*. The positions of wild type (*WT*) and mutant (*Mut*) allele-specific genotyping primer sets are indicated by *arrows*. *Bar*, 1 kilobase. *B*, multiplex genotyping PCR of DNA isolated from wild type (+/+), heterozygous (+/−), and homozygous mutant (−/−) mice using both wild type- and mutant-specific primer pairs showing detection of wild type (196 bp) and mutant (367 bp) alleles. *C*, Northern blot hybridization of total RNA from spinal cord (*sc*) and brain (*b*). The blot was hybridized with a ^{32}P-labeled cDNA probe complementary to exons 3 to 4 of the WARP transcript, then stripped and reprobed for β-actin as a loading control. *D*, duplicate Western blots of sciatic nerve guanidine hydrochloride extracts probed with a sheep anti-WARP polyclonal antibody or with a β-actin monoclonal antibody. Migration positions of molecular weight markers (kDa) are indicated on the *right*. *E*, immunofluorescence staining for WARP in sections of sciatic nerve using a rabbit anti-WARP VWA domain polyclonal antibody. *Bar*, 100 μm.

Nerve Function Abnormalities in WARP-null Mice—To determine any phenotypic consequences of WARP deficiency that were not apparent in routine observations, wild type and mutant mice were compared using a series of motor function and behavioral tests. Spontaneous activity of WARP-null mice on the running wheel and in locomotor activity tests was the same as wild type, and muscle strength measured by the grip strength test was unaffected (data not shown). Both wild type and knock-out mice demonstrated a similar performance in the rotarod, a test of sustained coordinated movements, independent of the degree of task difficulty (data not shown), suggesting that there are no disturbances in general motor function of WARP-null mice. However, homozygous WARP-null mice performed more poorly than wild type mice in the ledged beam test, a measure of fine motor coordination and balance. Although WARP-null mice showed no difference in the number of steps taken on the ledged beam in the last 33 cm where measurements were recorded, the knock-out mice demonstrated a significant increase in the distance marker of initial foot fault (Fig. 2*A*, $p < 0.05$), indicating that the mutant mice had their initial foot fault at a point where the beam was wider. The mutant mice had significant increases in the number of foot faults for right front ($p = 0.03$) and right hind ($p = 0.04$) paws. Moreover, an increase in the number of foot faults for the left hind paw was observed, but this was not statistically significant compared with the wild type (Fig. 2*B*). In addition, homozygous WARP-null mice also performed more poorly on the hotplate test, demonstrating that WARP knock-out mice have an increased latency to respond to a painful stimulus (Fig. 2*C*, $p < 0.01$) compared with wild type mice. Taken together, these data indicate that WARP-null mice do not exhibit general disturbance to their motor function, but their fine motor coordination and their response to acute painful stimulus is impaired.

Collagen VI Disorganization in WARP-null Peripheral Nerves—WARP has been recently identified as a component of the endoneurial basement membrane in peripheral nerves (5) and has been demonstrated to interact with perlecan (3). We also investigated the potential interaction of WARP with type VI collagen, which shares an overlapping expression pattern with WARP in peripheral nerves, in skeletal muscle, and in the chondrocyte pericellular matrix. Recombinant WARP was tested for its ability to bind collagen VI purified from bovine cornea by surface plasmon resonance analysis using a Biacore 3000 system.

Injection of recombinant WARP at 94, 187, 375, and 750 nM showed binding to immobilized collagen VI in a dose-dependent manner (Fig. 3*A*). After the end of injection no dissociation was observed, indicating that a stable complex was formed. To further validate the interaction, reciprocal binding was shown by injecting collagen VI at 120 μg/ml over WARP immobilized to a CM5 sensor chip (Fig. 3*B*). Although both WARP and collagen VI contain VWA domains with MIDAS (metal ion-dependent adhesion site) sequences, all injections were performed in the presence of EDTA, indicating that the interaction between collagen VI and WARP is not dependent on cations.

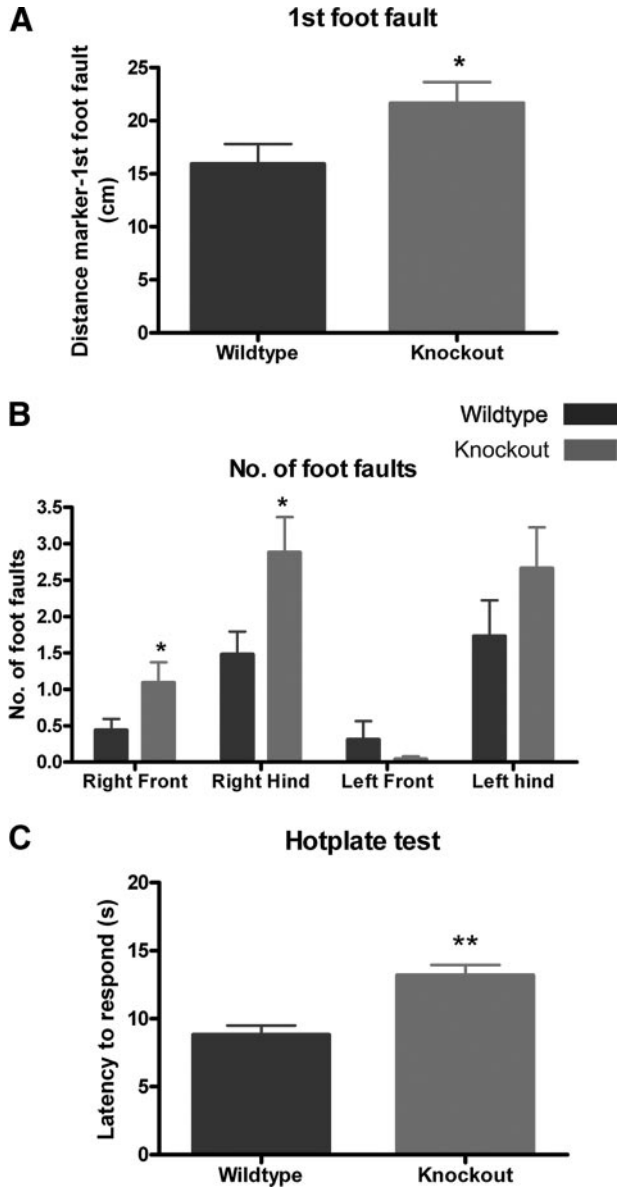

FIGURE 2. **Nerve function abnormalities in WARP-null mice.** *A*, first foot fault in the ledged beam test. Data are expressed as the average distance marker at which point the initial foot fault occurs for wild type ($n = 12$) and WARP-null mice ($n = 12$) mice on the ledged beam test. Independent sample *t* test: *, $p < 0.05$ *versus* wild type. *B*, number of foot faults in the ledged beam test. Data are expressed as the average number of foot faults for the four paws for wild type ($n = 12$) and WARP-null mice ($n = 12$) mice on the ledged beam test. Independent sample *t* test: *, $p < 0.05$. *C*, assessment of acute pain perception on the hotplate. Data are expressed as latency to respond (*s*) means ± S.E. of the mean for wild type ($n = 12$) and homozygous WARP-deficient ($n = 12$) mice. Independent sample *t* test: **, $p < 0.01$.

Kinetic data for the interaction was obtained by injecting WARP at 2000 and 1000 nM over immobilized collagen VI. Local fitting of the interaction between collagen VI and WARP using the Langmuir 1:1 binding model generated a K_D of 35 nM ($\chi^2 = 0.215$) and 32 nM ($\chi^2 = 0.401$) respectively, indicating a high affinity interaction between these two proteins.

Because collagen VI and perlecan both interact with WARP and WARP is a structural component of the peripheral nerve ECM, we analyzed the distribution of perlecan and collagen VI in nerves of wild type and WARP-null mice. Immunofluorescence staining of sciatic nerve sections revealed that collagen VI was significantly reduced in WARP-null mice (Fig. 4*B*) compared with wild type (Fig. 4*A*). Analysis by confocal laser scanning microscopy demonstrates that collagen VI immunolabeling is barely detectable when images from mutant mice were captured using identical exposure and gain settings as those for wild type mice (Fig. 4, *A* and *B*). Visualization of the collagen VI distribution in the mutant nerve by increasing the gain and exposure reveals that, in addition to a reduction in collagen VI immunostaining intensity, the collagen VI network is severely disorganized, and the fine sheet-like distribution normally present in the wild type nerve (Fig. 4*A*) is lost (Fig. 4*C*). The abnormal distribution of collagen VI in WARP-deficient nerve tissue was confirmed by immunohistochemistry using three independent collagen VI antibodies raised to purified human cartilage collagen VI, to recombinant α1(VI) chain, and to human pepsinized collagen VI (data not shown). However, the endoneurial basement membrane was not affected, as immunolocalization for perlecan (Fig. 4*D*) and laminin (data not shown) in WARP-null mice was indistinguishable from wild type mice. The collagen VI distribution in the outer perineurium layer of the nerve, where WARP is not expressed (5), was also unaffected in the mutant mice (Fig. 4, *E* and *F*). These data demonstrate that the basement membranes surrounding myelinated axons in WARP-null peripheral nerves are intact, but the microfibrillar collagen VI matrix is disrupted in the endoneurium.

Ultrastructural Abnormalities in WARP-null Peripheral Nerves—To examine the effects of WARP deficiency on the sciatic nerve morphology in more detail, electron microscopy was performed. In transverse sections of wild type mice sciatic nerve, the myelinated axons are clearly delineated by the interaxonal space (Fig. 5*A*). This space is filled with collagen I fibrils that separate the distinct basement membranes of neighboring axons (Fig. 5, *C* and *E*). In the mutant mice the distribution of interstitial collagenous matrix in the interaxonal space is altered (Fig. 5*D*) and appears to be less tightly associated to the basement membranes compared with wild type mice (Fig. 5*C*). Collagen VI microfibrils are not resolved in these electron micrographs from control or WARP-null mice. Although the ultrastructural analysis confirms that sciatic nerve endoneurial basement membranes are present in the WARP-null mice (Fig. 5, *D* and *F*), unusual focal fusions of the distinct basement membranes of neighboring axons are apparent in WARP-null nerves (Fig. 5, *D* and *F*; *arrows*), which were not detected in wild type mice (Fig. 5, *A*, *C*, and *E*). Although the ECM defects in WARP-deficient nerve were apparent, no evidence of demyelination or axonal degeneration could be detected by electron microscopy, and teased analysis did not reveal any abnormalities such as shortened or thinned internodal segments (data not shown).

Normal Skeletal Development and Musculature of WARP-deficient Mice—Given that the peripheral nerve interstitial matrix was severely disrupted in WARP-null mice, we sought to investigate the organization of other WARP-deficient tissues by examining the deposition of the WARP-interacting ligands collagen VI and perlecan. In tibial articular cartilage, WARP is restricted to the chondrocyte pericellular matrix in wild type mice (Fig. 6*A*) but was undetectable in homozygous mutant

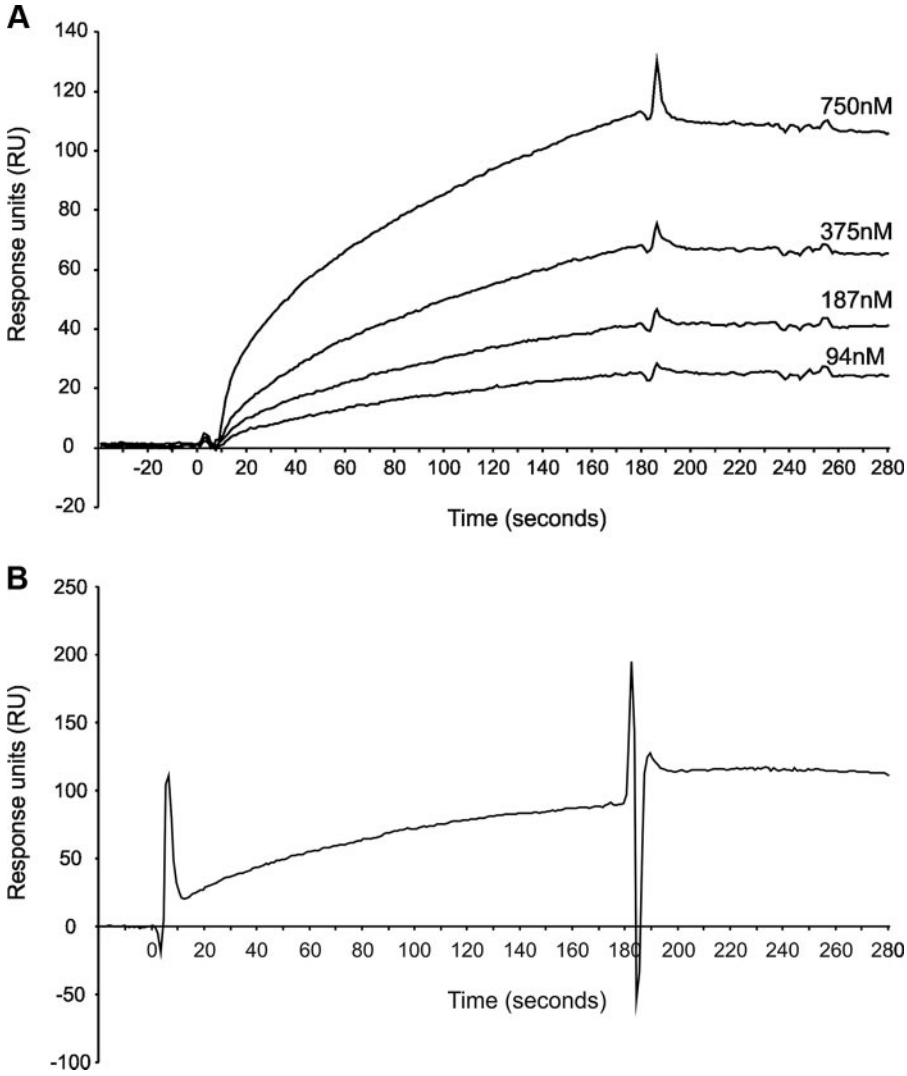

FIGURE 3. **Analysis of collagen VI-WARP interaction by surface plasmon resonance.** *A*, purified WARP diluted in HEPES-buffered saline buffer (94–750 nM) was injected over collagen VI immobilized to a CM5 sensor chip at 5 μl/min. Binding of WARP to collagen VI is apparent during the association phase. No loss of binding is observed during the dissociation phase, indicating the formation of a stable complex. *B*, reciprocal binding plot showing WARP immobilized to a CM5 sensor chip interacting with collagen VI (120 μg/ml) at 5 μl/min.

mice (Fig. 6*B*). The distribution of perlecan (Fig. 6, *C* and *D*) and of collagen VI (Fig. 6, *E* and *F*) in the chondrocyte pericellular matrix was unaltered in the absence of WARP, with no apparent abnormalities such as fragmentation, diffusion, or reduction in staining detected. Consistent with these findings, skeletal tissues of WARP-null mice developed normally, with no apparent malformations or size differences from wild type mice (Fig. 7, *A* and *B*). In particular, no abnormalities in joint formation or separation of developing skeletal structures were detected (Fig. 7, *C* and *D*) or in the formation of permanent cartilage structures such as the intervertebral discs (Fig. 7, *E* and *F*), meniscus, and sternum where WARP is normally expressed. In addition, sections of articular cartilage and intervertebral disc from 12-month-old wild type and WARP-deficient mouse tissues stained with toluidine blue revealed that WARP-null mice do not exhibit an increased susceptibility to joint pathology or to degeneration of the intervertebral disc compared with wild type mice (Fig. 7, *G–J*). These data indicate that WARP is dispensable for the normal development and function of skeletal tissues.

Our recent data have also demonstrated that WARP is a component of basement membrane structures surrounding muscle fibers (5). Histological analysis of skeletal muscle (Fig. 8, *A* and *B*) and diaphragm (data not shown) from wild type and WARP-null mice up to 12 months of age failed to demonstrate any gross histological changes consistent with muscle pathology. Immunostaining for collagen VI in sections of skeletal muscle revealed that collagen VI is still a prominent component of the endomysium surrounding WARP-deficient muscle fibers (Fig. 8, *C* and *D*), and the distribution of perlecan and laminin was also unaltered (data not shown). These data suggest that WARP is not critical for the assembly or stabilization of these matrix molecules in skeletal muscle or cartilage and provide further evidence for the tissue specificity of the ECM defect in peripheral nerves.

DISCUSSION

We have generated mice deficient in the ECM molecule WARP to help elucidate its function in skeletal tissues and in basement membranes. WARP has previously been shown to interact specifically with perlecan (3), and we also demonstrate here that WARP forms high affinity interactions with collagen VI, suggesting a potential function in bridging ECM networks. Mice deficient in WARP develop normally and have no detectable abnormalities of basement membrane formation or in musculoskeletal development. However, the ablation of WARP expression disrupts the association of collagen VI and interstitial collagen fibrils with the endoneurial basement membrane of peripheral nerves, indicating an important function for WARP in the organization of nerve connective tissues.

Ultrastructural studies have previously demonstrated that collagen VI microfibrils associate with interstitial fibrillar collagens in the endoneurium (15) and in other tissues (16) and are often found particularly concentrated adjacent to basement membranes (15, 17), suggesting a function in anchoring between these ECM structures. Our data indicate that WARP may facilitate the linkage between collagen VI and basement membrane molecules such as perlecan and

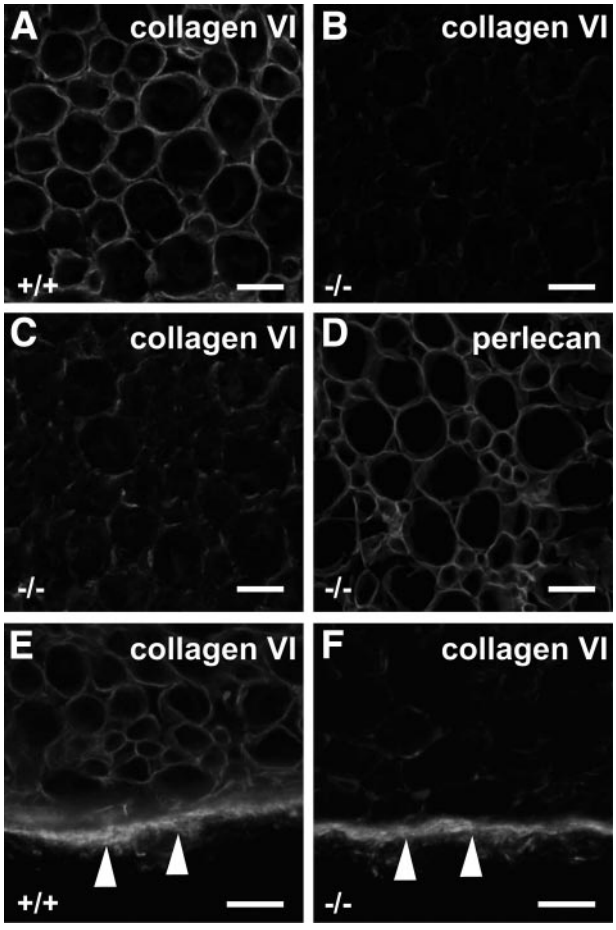

FIGURE 4. **Confocal analysis of sciatic nerve endoneurial matrix in wild type and WARP-null mice.** Immunofluorescent staining for collagen VI is significantly weaker in WARP-deficient mice (*B*) than in wild type (*A*) mice. Visualization of the field in image B with increased gain (*C*) reveals that the collagen VI matrix is disorganized as well as reduced in the WARP-null mouse. Perlecan still forms an intact basement membrane structure in the WARP-deficient endoneurium (*D*). The collagen VI structures in the outer perineurium layer (*arrowheads*) are unaffected in the WARP knock-out (*F*) compared with the wild type (*E*) mouse. *Bar*, 10 μm.

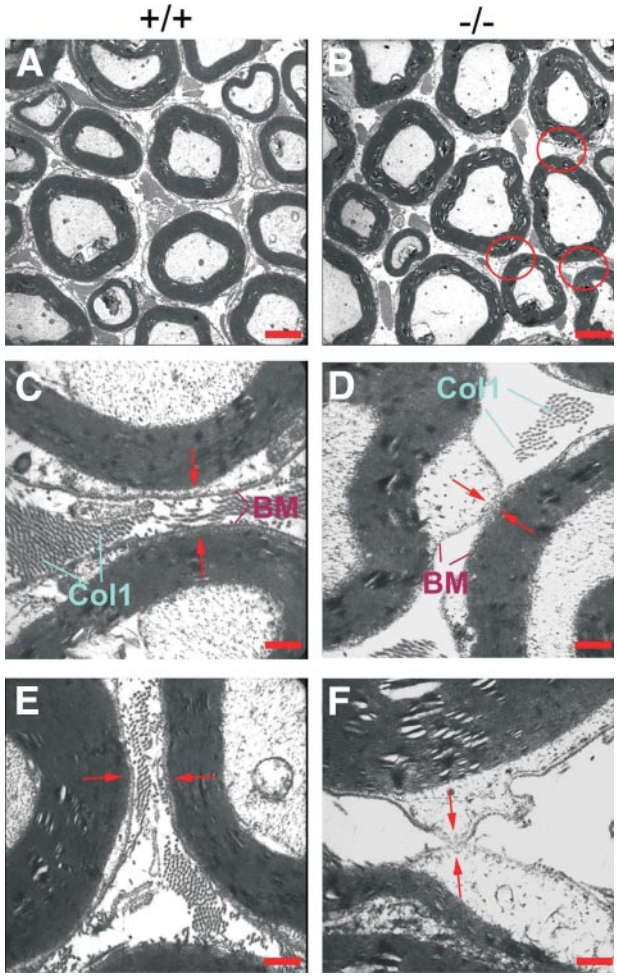

FIGURE 5. **Basement membranes of adjacent axons in the sciatic nerve are partially fused in mutant mice.** Ultrastructural analysis of transverse sections from the sciatic nerve isolated from wild type (*A*, *C*, and *E*) and WARP -null mice (*B*, *D*, and *E*). Overviews (*A* and *B*) and higher magnifications (*C–F*) of several axons are shown, and areas of interest are indicated by *circles* (*B*). Basement membranes (*BM*) of axons in wild type mice are separated by an inter-axonal space filled with bundles of collagen I fibrils (*Coll*). *Arrows* highlight the alignment of the basement membranes in wild type and mutant mice. *Bar*, 2.8 μm (*A* and *B*), 460 nm (*C–E*), 350 nm (*F*).

that the absence of WARP disrupts this interaction in nerves resulting in ECM disorganization and subsequent fusion of adjacent basement membranes.

However, the structure of the collagen VI networks in the other tissues examined appeared normal in the absence of WARP, suggesting that WARP does not have a critical role in stabilizing the ECM localization of collagen VI in cartilage and muscle. The interaction of WARP with collagen VI, its co-expression in skeletal muscle, and the known role of collagen VI mutations in human muscular dystrophies (18) prompted us to examine skeletal muscle histology and the muscle collagen VI matrix. However, unlike in nerve, WARP-deficient mice formed an apparently normal collagen VI matrix in muscle and showed no histological or behavioral evidence of muscle pathology, providing further evidence for the tissue specificity of the ECM disruption observed in nerve.

A potential reason for this apparent tissue-specific effect is that collagen VI has been shown to form different structures in different tissues (15), and these may require the participation of interacting molecules as co-factors in their assembly or integration into the surrounding ECM. One such molecule is biglycan, which has been demonstrated to catalyze the assembly of collagen VI into specific structural networks in *in vitro* assays (19). The ECM molecule Fras1 is predicted to bind collagen VI via a domain with high homology to the collagen VI binding domain of chondroitin sulfate proteoglycan NG2 (20) and provides another example of a molecule with an essential role in anchoring collagen VI within specific ECM structures. In mice deficient in Fras1 (20) or in GRIP1, which is essential for correct processing and localization of Fras1 (21), there is a loss of collagen VI deposition in the dermal-epidermal junction but not in the underlying interstitial matrix. It is, therefore, possible that WARP is a critical co-factor for the assembly or integration of the endoneurium-specific structural form of collagen VI in nerves.

Another possible mechanism for the nerve-specific collagen defect in WARP-null mice is that other tissues may have a higher turnover of ECM molecules and, therefore, a greater capacity to repair defective tissue structures. Many nerve ECM

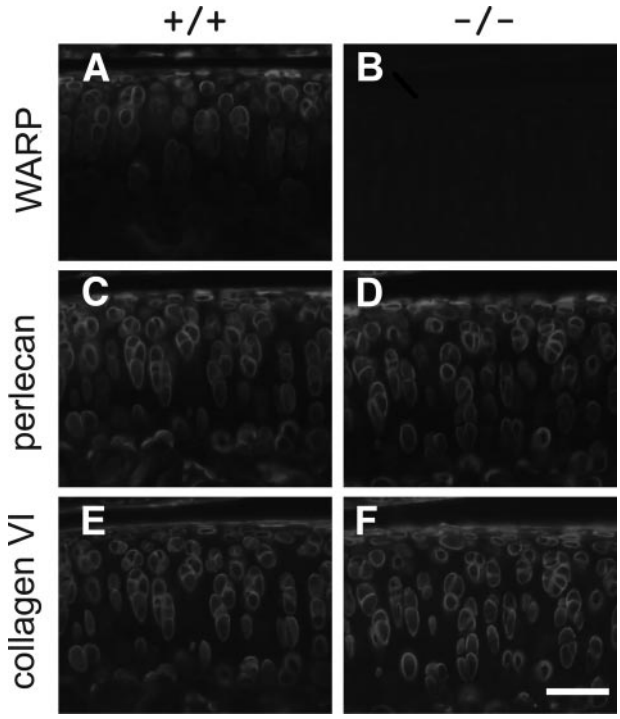

FIGURE 6. **The distribution of WARP ligands in articular cartilage from WARP-null (−/−) and wild type (+/+) littermates is unaltered.** WARP was undetectable in the mutant mouse tissues (*B*) but was present in the chondrocyte pericellular matrix in articular cartilage of wild type mice (*A*). The distribution of perlecan (*C* and *D*) and collagen VI (*E* and *F*) was no different between wild type and WARP-null tissues. *Bar*, 50 μm.

molecules such as WARP (5), laminins (22), and nidogens (23) are expressed highly during early development and myelination but are down-regulated at the transcriptional level in adult nerve tissues except in response to injury (22, 23). A disorganization of collagen networks in nerve, therefore, may not necessarily undergo repair because it is not severe enough to compromise many normal functions. WARP-deficient mice with a disrupted collagen matrix develop normally and perform well in most motor function tests, but the nerve defect may only become apparent in stressful or demanding situations, such as acute nociceptive response like the hotplate test or when fine motor coordination and balance are required as demonstrated with the ledged beam test.

WARP has a striking expression pattern in skeletal development in that it is specifically expressed at sites of joint formation and articular cartilage rather than in cartilaginous structures that are replaced by bone through endochondral ossification (3), which suggests specific functions in joint cavitation and articular cartilage formation. However, the skeletal development of WARP-null mice is indistinguishable from wild type mice, and in particular, joints specify normally, and no abnormalities or delays in joint cavitation occur. It is likely that other molecules compensate for the loss of WARP; however, careful searching of mouse and human databases has failed to identify any homologues of WARP. Bioinformatic analysis has suggested that WARP may share an evolutionary relationship with the FACIT collagens XII and XIV based on sequence similarity, domain organization, and chromosomal location on regions of synteny (24). Notably, collagen XII has an overlapping expression pattern with WARP in developing articular cartilage (25); however, no compensatory increase in collagen XII immunostaining could be detected in WARP-deficient mice (data not shown).

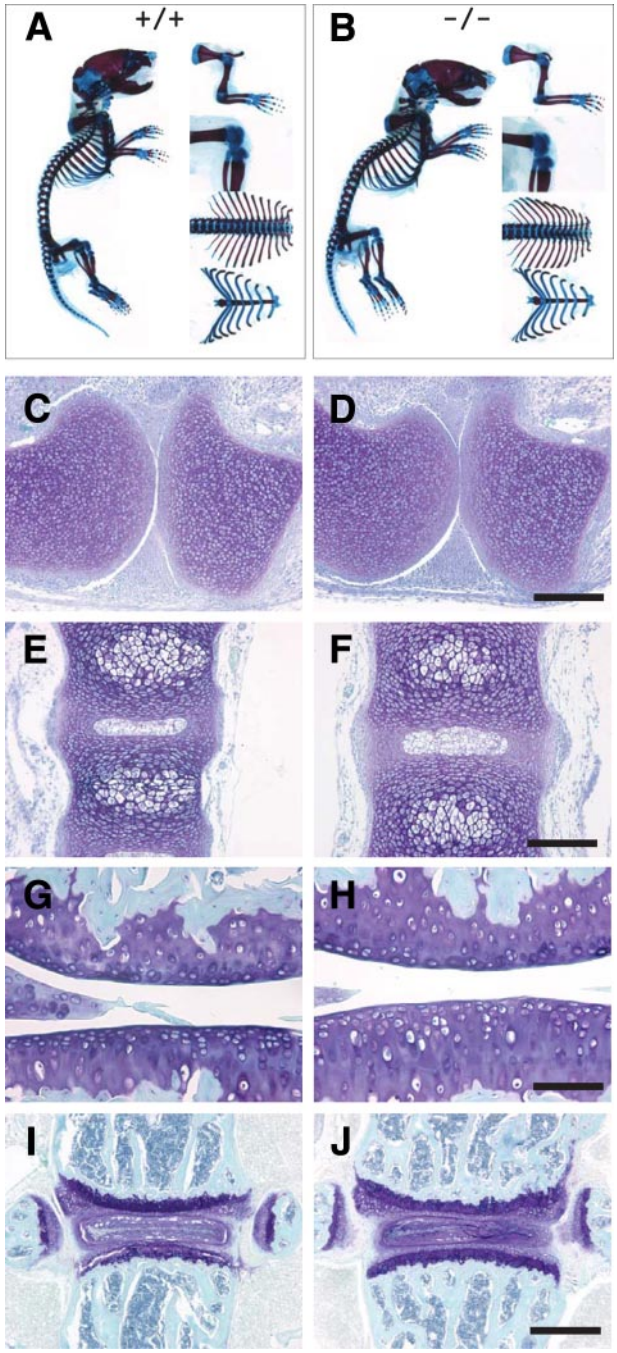

FIGURE 7. **Normal skeletal morphology of WARP-null mice.** Whole skeletal preparations of newborn WARP-deficient (*B*; −/−) and wild type (*A*; +/+) littermates were stained with Alcian blue and Alizarin red to stain cartilage tissues and bone structures, respectively, indicating that no gross skeletal malformations are apparent. Toluidine blue staining of E16.5 embryonic knee joints (*C* and *D*) and spines (*E* and *F*) shows normal development of skeletal structures with no apparent abnormalities. Sections of tibial articular cartilage (*G* and *H*) and intervertebral disc (*I* and *J*) of 12-month-old mice demonstrate normal tissue morphology and no evidence of degeneration. *Bar*, 200 μm (*C–F*), 100 μm (*G* and *H*), 500 μm (*I* and *J*).

In mature articular cartilage, WARP has a highly restricted localization in the chondrocyte pericellular

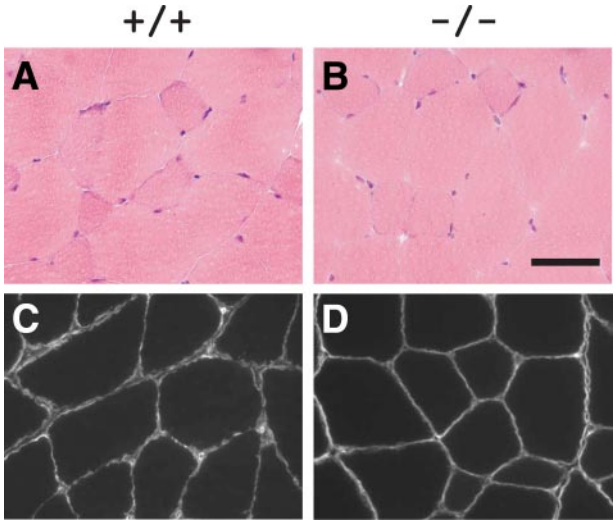

FIGURE 8. **Normal skeletal muscle in WARP-deficient mice.** *A*, representative cryosections of snap-frozen gastrocnemius muscle from 12-month-old WARP-null (*B*; −/−) and wild type (*A*; +/+) littermates stained with hematoxylin and eosin show normal muscle structure of the mutant mice. No signs of muscle degeneration or remodeling were detected. Immunostaining for collagen VI was present in the endomysium surrounding muscle fibers in both mutant (*D*) and wild type (*C*) mice. *Bar*, 50 μm.

matrix, a structure with important roles in facilitating cell-matrix interactions and in maintaining cartilage homeostasis, particularly in detecting and responding to changes in mechanical stimuli (26, 27). We predicted that ablating WARP expression would disrupt the pericellular matrix, which may alter interactions of chondrocytes with their surrounding matrix and, potentially, their response to mechanical forces. However, WARP-deficient cartilage tissues developed normally, retained an apparently normal pericellular matrix, and did not exhibit any signs of age-related pathology, indicating that WARP is not an essential component of the chondrocyte pericellular matrix. Given that the major components of the chondrocyte pericellular matrix, perlecan and collagen VI, are still intact in WARP-deficient cartilage, the putative role for WARP in linking matrix structures may be efficiently compensated for by other molecules. There are many examples of cartilage ECM molecules for which knock-out mice exhibit only mild or no deleterious effects on skeletal development, including COMP, matrilins, and others (for review, see Ref. 14). However, mutations in such molecules cause skeletal dysplasias, indicating that dominant negative effects of mutant proteins can often have more severe effects than the absence of ECM structural components. The possibility remains that WARP-null mice may exhibit defects in chondrocyte-matrix interactions that are not apparent under normal conditions but that may impair the response of WARP-deficient cartilage to pathologic conditions, as the pericellular matrix is known to undergo extensive remodeling in osteoarthritis (for review, see Ref. 27). It may, therefore, be informative to determine whether WARP-null mice have an increased susceptibility to cartilage damage when exposed to challenges such as increased load bearing or *in vivo* models of arthritis.

Our studies demonstrate that WARP deficiency causes a tissue-specific disruption of the ECM in peripheral nerves and results in defects in fine motor coordination and nociception. Although Schwann cell basement membranes appear to form normally, their associated interstitial collagen matrix is severely reduced and mislocalized, and the basement membranes of adjacent Schwann cells undergo abnormal fusion. These data suggest a specific function for WARP in bridging ECM networks important for stabilizing the peripheral nerve matrix. The observed ECM abnormalities and the resulting compromised nerve function are the first description of the results of WARP deficiency. Currently there are no human diseases known to be caused by mutations in the *Vwa1* gene encoding WARP, but these findings may help identify disorders that could result from mutations in this gene.

Acknowledgments—We gratefully acknowledge the mouse husbandry support provided by staff at the Murdoch Children's Research Institute as well as Dr. Matt Burton for confocal microscopy support.

REFERENCES

1. Whittaker, C. A., and Hynes, R. O. (2002) *Mol. Biol. Cell* **13,** 3369–3387
2. Fitzgerald, J., Ting, S. T., and Bateman, J. F. (2002) *FEBS Lett.* **517,** 61–66
3. Allen, J. M., Bateman, J. F., Hansen, U., Wilson, R., Bruckner, P., Owens, R. T., Sasaki, T., Timpl, R., and Fitzgerald, J. (2006) *J. Biol. Chem.* **281,** 7341–7349
4. Kvist, A. J., Nystrom, A., Hultenby, K., Sasaki, T., Talts, J. F., and Aspberg, A. (2008) *Matrix Biol.* **27,** 22–33
5. Allen, J. M., Brachvogel, B., Farlie, P. G., Fitzgerald, J., and Bateman, J. F. (2008) *Matrix Biol.* **27,** 295–305
6. Hallmann, R., Horn, N., Selg, M., Wendler, O., Pausch, F., and Sorokin, L. M. (2005) *Physiol. Rev.* **85,** 979–1000
7. Yurchenco, P. D., Amenta, P. S., and Patton, B. L. (2004) *Matrix Biol.* **22,** 521–538
8. LeBleu, V. S., Macdonald, B., and Kalluri, R. (2007) *Exp. Biol. Med.* (*Maywood*) **232,** 1121–1129
9. Erickson, A. C., and Couchman, J. R. (2000) *J. Histochem. Cytochem.* **48,** 1291–1306
10. Sambrook, J., and Russell, D. W. (2001) *Molecular Cloning: A Laboratory Manual*, 3rd Ed., Sections 7.4–7.8, Cold Spring Harbor Laboratory Press, Cold Spring Harbor, NY
11. Tillet, E., Wiedemann, H., Golbik, R., Pan, T. C., Zhang, R. Z., Mann, K., Chu, M. L., and Timpl, R. (1994) *Eur. J. Biochem.* **221,** 177–185
12. von der Mark, H., Aumailley, M., Wick, G., Fleischmajer, R., and Timpl, R. (1984) *Eur. J. Biochem.* **142,** 493–502
13. Brachvogel, B., Moch, H., Pausch, F., Schlotzer-Schrehardt, U., Hofmann, C., Hallmann, R., von der Mark, K., Winkler, T., and Poschl, E. (2005) *Development* **132,** 2657–2668
14. Aszodi, A., Legate, K. R., Nakchbandi, I., and Fassler, R. (2006) *Annu. Rev. Cell Dev. Biol.* **22,** 591–621
15. Keene, D. R., Engvall, E., and Glanville, R. W. (1988) *J. Cell Biol.* **107,** 1995–2006
16. Keene, D. R., Ridgway, C. C., and Iozzo, R. V. (1998) *J. Histochem. Cytochem.* **46,** 215–220
17. Kuo, H. J., Maslen, C. L., Keene, D. R., and Glanville, R. W. (1997) *J. Biol. Chem.* **272,** 26522–26529
18. Lampe, A. K., and Bushby, K. M. (2005) *J. Med. Genet.* **42,** 673–685
19. Wiberg, C., Heinegard, D., Wenglen, C., Timpl, R., and Morgelin, M. (2002) *J. Biol. Chem.* **277,** 49120–49126
20. Vrontou, S., Petrou, P., Meyer, B. I., Galanopoulos, V. K., Imai, K., Yanagi, M., Chowdhury, K., Scambler, P. J., and Chalepakis, G. (2003) *Nat. Genet.* **34,** 209–214
21. Takamiya, K., Kostourou, V., Adams, S., Jadeja, S., Chalepakis, G., Scambler, P. J., Huganir, R. L., and Adams, R. H. (2004) *Nat. Genet.*

36, 172–177
22. Wallquist, W., Patarroyo, M., Thams, S., Carlstedt, T., Stark, B., Cullheim, S., and Hammarberg, H. (2002) *J. Comp. Neurol.* **454,** 284–293
23. Lee, H. K., Seo, I. A., Park, H. K., Park, Y. M., Ahn, K. J., Yoo, Y. H., and Park, H. T. (2007) *J. Neurochem.* **102,** 686–698
24. Fitzgerald, J., and Bateman, J. F. (2003) *FEBS Lett.* **552,** 91–94
25. Gregory, K. E., Keene, D. R., Tufa, S. F., Lunstrum, G. P., and Morris, N. P. (2001) *J. Bone Miner. Res.* **16,** 2005–2016
26. Guilak, F., Alexopoulos, L. G., Upton, M. L., Youn, I., Choi, J. B., Cao, L., Setton, L. A., and Haider, M. A. (2006) *Ann. N. Y. Acad. Sci.* **1068,** 498–512
27. Poole, C. A. (1997) *J. Anat.* **191,** 1–13